

DOI: 10.1002/cmdc.200600242

# Homology Modeling of the Serotonin Transporter: Insights into the Primary Escitalopram-binding Site

Anne Marie Jørgensen,<sup>[a, b]</sup> Lena Tagmose,<sup>[b]</sup> Anne Marie M. Jørgensen,<sup>[b]</sup> Sid Topiol,<sup>[c]</sup> Michael Sabio,<sup>[c]</sup> Klaus Gundertoft,<sup>[b]</sup> Klaus P. Bøgesø,<sup>[d]</sup> and Günther H. Peters<sup>\*[a]</sup>

*The serotonin transporter (SERT) is one of the neurotransmitter transporters that plays a critical role in the regulation of endogenous amine concentrations and therefore is an important target for therapeutic agents affecting the central nervous system. The recently published, high resolution X-ray structure of the closely related amino acid transporter, Aquifex aeolicus leucine trans-*

*porter (LeuT), provides an opportunity to develop a three-dimensional model of the structure of SERT. We present herein a homology model of SERT using LeuT as the template and containing escitalopram as a bound ligand. Our model explains selectivities known from mutational studies and varying ligand data, which are discussed and illustrated in the paper.*

## Introduction

Selective serotonin reuptake inhibitors (SSRIs) are drugs of choice for the treatment of major depressive disorders, obsessive-compulsive disorder, and anxiety disorders. Well-known examples of SSRIs on the market are escitalopram (*S*-citalopram, also an allosteric serotonin reuptake inhibitor (ASRI));<sup>[1]</sup> trade names Cipralext, Lexapro), fluoxetine, paroxetine, and sertraline.<sup>[2–5]</sup> The target of SSRIs is the highly evolutionarily conserved serotonin transporter (SERT) that regulates serotonergic neurotransmission by modulating serotonin (5-HT) concentration in the synapse.<sup>[6,7]</sup> SSRIs affect the concentration of the neurotransmitter serotonin (5-HT) by inhibiting the reuptake of the neurotransmitter into nerve cells.<sup>[8]</sup> Despite the fact that the serotonin transporter has drawn major interest in the CNS-focused pharmaceutical industry, research activities are hampered by the lack of a three-dimensional protein structure.

A three-dimensional model at the atomic level is an important tool to further characterize the protein and to give suggestions for site-directed mutagenesis. Residues in the transporter have been studied by mutagenesis, and various pharmacophore models have been constructed for SERT ligands, including models for the substrate<sup>[9]</sup> and reuptake inhibitors.<sup>[10–15]</sup> Results from such studies provide direct and indirect structural insight into the possible interaction patterns between ligands and the transporter. One of the constructed models is the SSRI pharmacophore model.<sup>[10]</sup> A characteristic of the model is that it describes ligand selectivity for the citalopram/talopram/talsupram compound class with respect to the norepinephrine transporter (NET) along with SERT ligand enantioselectivity. Further validation of the model has been obtained from mutagenesis studies, where residues critical for transporter functionality have been identified.<sup>[8,16–18]</sup> However, because of difficulties in distinguishing between direct and indirect effects of res-

idues on ligand-binding and transporter function, the actual interactions between for example, SERT ligands and the protein remain to be elucidated. Various homology models have previously been constructed. These were based on the X-ray structures of the distantly related *E. coli* transporters such as the Na<sup>+</sup>/H<sup>+</sup> antiporter NhaA and lactose permease structures (LacY).<sup>[19–21]</sup> Despite the fact that these proteins consist of 12  $\alpha$ -helical TM domains (like SERT<sup>[8]</sup>), they do not belong to the same family as SERT and their topology might therefore be different. Indeed, as observed by Ravna et al.,<sup>[21]</sup> a LacY-based SERT model cannot account for all residues in the ligand binding site that are known to be important for ligand binding.

The recent publication of an X-ray structure of a homologue of SERT, the bacterial leucine transporter (LeuT),<sup>[22]</sup> belonging to the same transporter family as SERT, offers an opportunity to build a more reliable model than was hitherto possible and to give suggestions as to specific protein–ligand interactions. LeuT functions in the bacterial plasma membrane where it couples the inward-oriented transport of the amino acid leu-

[a] A. M. Jørgensen, Assoc. Prof. G. H. Peters  
MEMPHYS-Center for Biomembrane Physics, Department of Chemistry, Technical University of Denmark, Building 206, 2800 Kgs. Lyngby (Denmark)  
Fax: (+45) 45-88-31-36  
E-mail: ghp@kemi.dtu.dk

[b] A. M. Jørgensen, L. Tagmose, A. M. M. Jørgensen, K. Gundertoft  
Department of Computational Chemistry, H. Lundbeck A/S, 9 Ottiliavej, 2500 Valby (Denmark)

[c] S. Topiol, M. Sabio  
Department of Computational Chemistry, Lundbeck Research USA, Inc, 215 College Road, Paramus, NJ 07652 (USA)

[d] Dr. K. P. Bøgesø  
Lundbeck Research Denmark, H. Lundbeck A/S, 9 Ottiliavej, 2500 Valby (Denmark)

cine to the sodium concentration across the membrane.<sup>[22]</sup> A similar transport mechanism is expected for other neurotransmitter sodium symporters (NSS).<sup>[23]</sup> LeuT has been crystallized in a substrate-occluded form, where the substrate leucine as well as two sodium ions are bound to partly overlapping sites located in the middle of the 12 transmembrane  $\alpha$ -helical domains.<sup>[22]</sup> Experimental<sup>[8,17]</sup> and sequence-based profile studies<sup>[24,25]</sup> suggest a similar topology for SERT. The X-ray structure of LeuT has been proposed to represent one of at least three different transporter conformations that are either open to the extracellular medium, closed (crystallographic solved structure), or open toward the intracellular medium. Opening and closing of an extra- and intracellular gate along with rotation or movements of some transmembrane domains have been proposed to regulate the substrate and ion accessibility to their corresponding binding sites.<sup>[22,26,27]</sup> Reuptake inhibitors such as the SSRIs are expected to inhibit transporter function by binding to the substrate-binding site,<sup>[8]</sup> resulting in transporter-inhibitor complexes that share conformational properties with the crystallized LeuT conformation.<sup>[22]</sup> Based on the LeuT structure, three models for the SERT apo protein have recently been described in the literature.<sup>[28–30]</sup> However, they do not provide detailed insight into protein–ligand interactions. Herein, we present a homology model of the human serotonin transporter (hSERT) in complex with the SSRI/ASRI escitalopram.

## Computational Methods

### Structural elements in LeuT and their relation to other NSS transporters

The LeuT leucine substrate is enclosed by residues from four transmembrane domains: TM1, 3, 6, and 8.<sup>[22]</sup> None of these domains has an ideal helical structure at the ligand-binding site: TM1 and 6 are partly unwound, whereas TM3 and 8 are bent in their center region. Residues N21, L25, G26 (TM1), V104, Y108 (TM3), F253, T254, S256, F259 (TM6), S355, and I359 (TM8) are in direct contact with the ligand, (cf. Table 1). The two sodium ions are coordinated by residues from TM1, 6, and 7 (Na1), and TM1 and 8 (Na2). In the corresponding region of the serotonin transporter, experimental results have suggested

that residues from transmembrane domains 1 and 3 are involved directly in ligand-binding in SERT,<sup>[8]</sup> whereas TM1 and TM7 residues may play a role in sodium-binding and/or translocation.<sup>[31]</sup> The SERT domains TM6 and TM8 still are not fully characterized. A comparison of sequences for NSS members has revealed that the presence/absence of an aspartic acid in TM1 categorizes NSS proteins as transporters for either amino acids or monoamines.<sup>[32]</sup> In the monoamine transporters, this aspartate (D98 in hSERT) is expected to coordinate ligands by an ion-reinforced hydrogen bond and has also been found to be important for coupling substrate transport to the sodium gradient.<sup>[22,33,34]</sup> In the NSS amino acid transporters, a glycine is located at this position.<sup>[32]</sup>

In the LeuT X-ray structure, a  $\text{Cl}^-$  ion was identified at the extracellular surface of the protein, which is located distally to the ligand- and sodium-binding sites.<sup>[22]</sup> The observed  $\text{Cl}^-$  binding site is not considered as the putative site to which chloride ions bind during the transport cycles, as residues coordinating to the ion are not conserved between various  $\text{Na}^+/\text{Cl}^-$ -dependent transporters. As a result of the lack of additional information about how  $\text{Cl}^-$  binds to the transporter, we do not focus on a  $\text{Cl}^-$  binding site in the present modeling study. Herein, we present the methodology and strategy for constructing our LeuT-based SERT model.

### Alignment

To examine the degree of residue conservation between the serotonin transporter and bacterial amino acid transporters, we implemented sequences for six mammalian serotonin transporters from various species: human (h), chicken (g), bovine (b), rat (r), mouse (m), drosophila (d), and two bacterial amino acid transporters: the *Aquifex aeolicus* leucine transporter (LeuT) and the *Symbiobacterium thermophilum* tryptophan transporter (TnaT) in the alignment construction (Figure 1). The primary sequences were obtained from the Swiss-Prot protein databank,<sup>[35]</sup> whereas the coordinates of the leucine transporter were acquired from the Protein Data Bank.<sup>[36]</sup> ClustalW<sup>[37]</sup> was used to generate the alignment. To avoid gaps in the membrane-transversing regions and to align residues that are expected to play a similar role in the template and in the monoamine transporters, constraints were included in the alignment procedure. The constraints were guided by comparing results from site-directed mutagenesis with the proposed function of specific residues in LeuT.

The constraints are summarized in Figure 2, and data that justify application of these constraints are listed in Table 2. This resulted in an alignment very similar to the alignment proposed by Yamashita et al.,<sup>[22]</sup> the only differences being the alignment of LeuT W481 and T482 in the sixth extracellular loop region.

### Molecular structure building

The overall modeling procedure applied here (outlined in Figure 2) involves three steps: 1) initial homology modeling, 2) initial ligand docking combined with model relaxation/ex-

**Table 1.** Corresponding LeuT and hSERT residues discussed in the text.

Conserved				Nonconserved			
TM	LeuT	hSERT	Ligand contact <sup>[a]</sup>	TM	LeuT	hSERT	Ligand contact
1	L25	L99	+/-	1	N21	Y95	+/+
1	G26	G100	+/+	1	G24	D98	-/+
3	Y107	Y175	-/+	3	P101	A169	-/+
3	Y108	Y176	+/+	6	T254	I172	+/+
6	F253	F335	+/+	6	T254	S336	+/-
6	F259	F341	+/+	6	S256	G338	+/+
8	S355	S438	+/+	6	L257	P339	-/-
				6	A261	V343	-/-
				8	I359	G442	+/+

[a] First and second sign refer to LeuT and hSERT, respectively (+: ligand contact; -: no ligand contact).



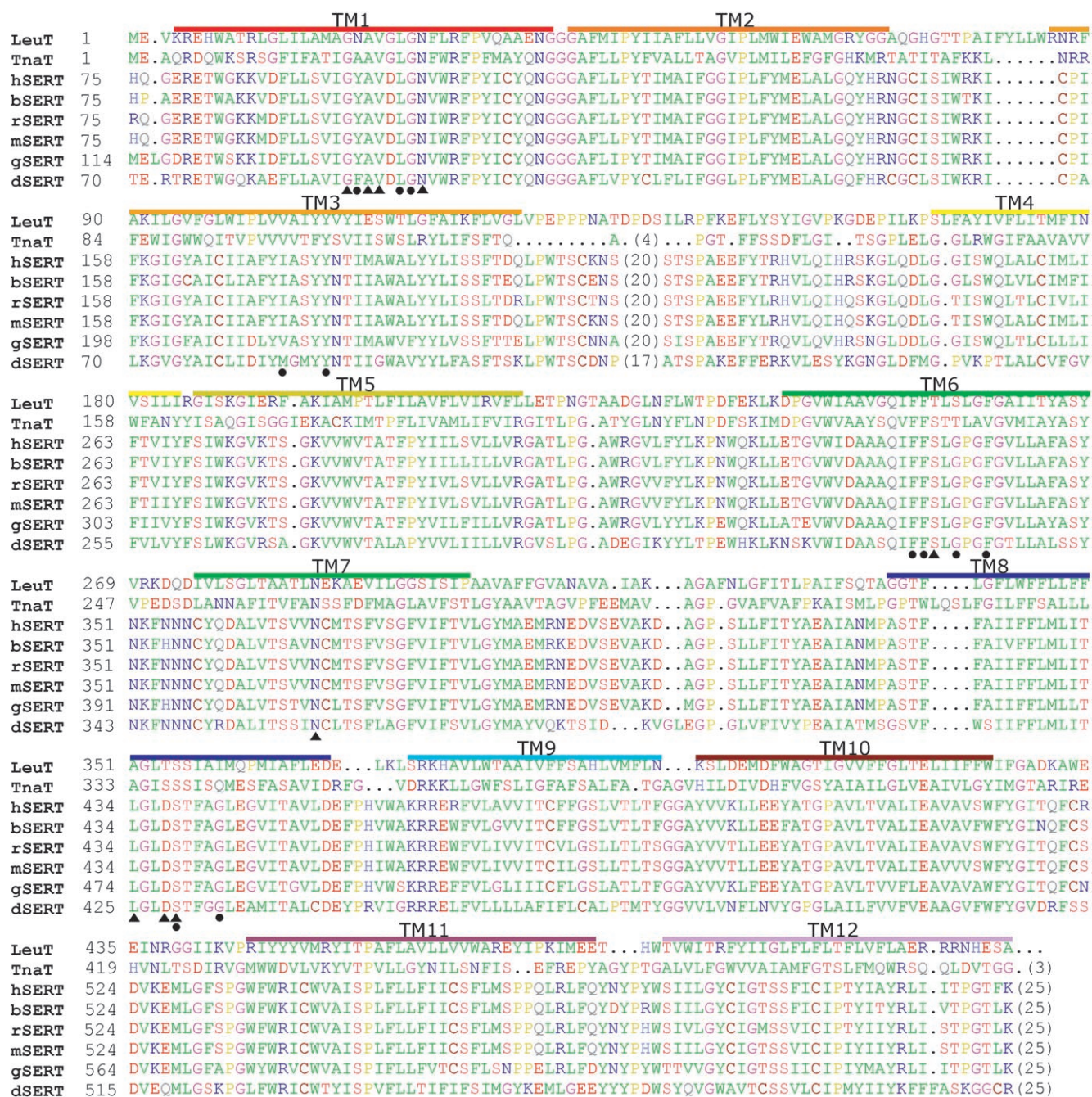
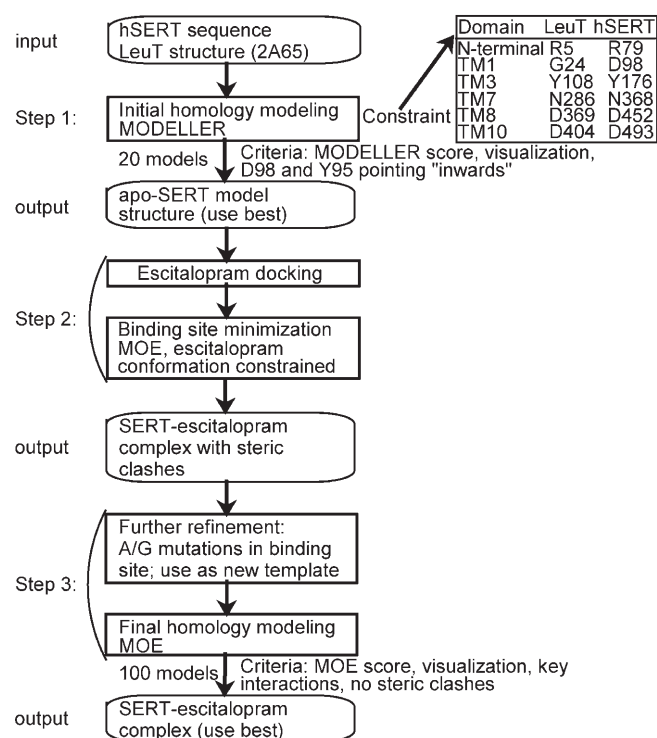


Figure 1. Alignment of sequences for bacterial amino acid transporters (LeuT and TnaT) and serotonin transporters from different mammalian species. Colored bars highlight the residues involved in transmembrane domains TM1–TM12. Circles and triangles indicate residues involved directly in ligand and sodium binding, respectively, in the LeuT X-ray structure and in our hSERT model.

pansion of the putative ligand-binding site, and 3) final homology modeling. The challenge in step 1 is to obtain and select a reasonable model. We used MODELLER 8v2<sup>[38]</sup> to generate 20 homology models of the hSERT apo protein structure, with MODELLER producing structures with penalties between 2700 and 5000; the lower the penalty, the better the model. In the best scoring models, unfavorable protein conformations were limited to regions for which no template structures are available. The best models at this stage differed primarily in side-chain conformations, whereas protein-backbone conformations

were almost identical to the original template. Model selection was guided by key information from mutagenesis studies<sup>[8,16,33]</sup> and pharmacophore modeling.<sup>[10]</sup> Mutagenesis studies have, for example, suggested contacts between escitalopram and residues Y95 and I172.<sup>[16,18]</sup> Hence, a model in which these two residues pointed inward towards a putative binding site was selected for further analysis. This model was also the best-ranking MODELLER model. As sodium ions and ligand were not included in the homology modeling step, residue D98 pointed outwards from the ligand- and sodium-binding sites. This resi-



**Figure 2.** Flowchart for the molecular modeling process. 2A65 is the PDB entry for LeuT.

using PROCHECK<sup>[40]</sup> and refined with respect to outliers in the Ramachandran plot using an energy minimization procedure (combination of Steepest Descent, Conjugate Gradient, and Truncated Newton) in MOE<sup>[41]</sup> and applying the MMFF94 force field and default settings.<sup>[42]</sup> During energy minimization, all residues except for those to which outliers were associated, were fixed in space. Residues N-terminal to R79 and C-terminal to K605 plus 20 residues (W204–H223) in the long, second extracellular loop region, for which no structural template is available, were not included in the subsequent modeling work. These three regions are expected to be distal to the ligand-binding site, and their presence or absence is therefore unlikely to affect the ligand-binding region.<sup>[43–45]</sup> Lastly, sodium ions (Na1, Na2) were introduced at positions corresponding to the ones in LeuT.

### Ligand docking

In step 2, ligands were introduced in the putative ligand-binding site in the hSERT model. Initially, the natural substrate 5-HT was docked manually into the preliminary hSERT model. The manual placement was made such that the amine–D98 interaction was established and the indole skeleton was located in a region in hSERT corresponding to the hydrophobic cleft in LeuT occupied by the leucine side chain. All docking attempts revealed that the volume available for ligand-binding was too small. Residues involved in the binding of escitalopram are more characterized than those for 5-HT.<sup>[16, 18, 33, 46]</sup> Therefore, we built our model with escitalopram. Escitalopram in its presumed bioactive conformation<sup>[10]</sup> was manually placed in the putative ligand-binding site in a position where its amine group could interact with D98 by an ion-reinforced hydrogen bond. The ligand propyl side chain was in hydrophobic contact with Y95, whereas the aromatic parts of the ligand interacted with I172. The selected position also gave rise to a direct contact between A169 and the phthalane group. Mutational studies suggest that all four residues are involved in escitalopram-binding.<sup>[16, 18, 33, 46]</sup> However, the putative binding pocket was in several respects too narrow for escitalopram and gave rise to steric clashes between the ligand and the protein. Manual side chain reorientations in the binding cleft were not sufficient to provide space for the ligand.<sup>[47]</sup> Hence, some backbone modifications were introduced. As the residues in and next to the unwound regions of TM1 (LeuT/hSERT residues N21/Y95, G24/D98) and TM6 (S256/L338, L257/P339, A261/V343) are not conserved between these two transporters, (cf. Table 1), the tight hydrogen-bonded network observed between some of these residues may differ between the two transporters (Table 3).

**Table 3.** Inter-helical contacts in the ligand-binding site in LeuT and hSERT.

Inter-helical contact	LeuT	hSERT
Ligand/TM1—TM3	Leucine ligand—Y108	D98—Y176
TM1—TM6	N21—S256	Y95—G338
TM1—TM8	N21—S355	Y95—S438

due is critical for ligand-binding and is expected to anchor ligands in the binding cleft in hSERT by an ion-reinforced hydrogen bond between a protonated ligand amine and its own carboxy group.<sup>[10, 33]</sup> To afford the most optimal contact to Na1 and the ligands, the D98 dihedral angle  $N-C_{\alpha}-C_{\beta}-C_{\gamma}$  was adjusted from  $-70^{\circ}$  to  $65^{\circ}$ , a side chain conformation which is also frequently observed in X-ray structures.<sup>[39]</sup> In this position, D98 pointed inward towards the putative ligand-binding site. The stereochemical quality of the model was further analyzed



Nonconserved residues in TM3 (for example LeuT/hSERT residues P101/A169, L102/F170, V103/Y171, V104/I172, I106/S174, V109/N177), and TM8 (for example LeuT/hSERT residue P362/G445) may also enable different conformations of these regions in different transporters. Therefore, the backbone conformation in TM1 (G95-G100), TM3 (A167/A181), TM6 (L331-V343), and TM8 (A437-G445) was modified as follows:<sup>[48]</sup> backbone conformational changes were achieved by first introducing escitalopram manually in its presumed bioactive conformation<sup>[10]</sup> in the proposed ligand-binding site.<sup>[16,18,33,49,50]</sup> In this binding mode, there were several steric clashes between the protein and the ligand. Next, the backbone conformation was changed by energy minimization (same procedure as described above), where conformational changes were limited to the above-mentioned regions and to side chains of residues located within 8.5 Å of the ligand. Constraints on all ligand torsions and on the D98—ligand amine salt bridge ensured that the ligand conformation and orientation were maintained.

To remove adverse interactions, a second round of homology modeling was performed in step 3 using the relaxed hSERT-escitalopram model as a starting point. Residues in the active site that are not conserved between SERT and LeuT or can be expected to adopt different conformations in different transporters were mutated to alanine or glycine (glycine if the residue is already alanine): Y95 A, L99A, W103A, I168A, A169G, F170A, Y175A, Y176A, N177A, T178A, I179A, F334A, F335A, F341A, V343A, L443A, and T497A. The resulting model structure was then used as a structural template. Additionally, escitalopram and the two sodium ions Na1 and Na2 were included as a MOE environment.<sup>[41]</sup> Applying this tool, the homology model was built around these elements. The final model was refined by energy minimization (same methodology as described above) in MOE. Finally, the model including the ligand was subjected to a brief relaxation using the Protein Preparation module in Maestro (default settings applied).<sup>[51]</sup> This is a two-part procedure that consists of optimizing hydroxyl and thiol torsions in the first stage, followed by an all-atom restrained impact minimization to relieve clashes<sup>[52]</sup> (OPLS force field<sup>[53]</sup>).

### Model validation

PROCHECK<sup>[40]</sup> was used to evaluate the quality of the constructed model. Within the 12 transmembrane domains, outliers that were identified by the MOE protein report<sup>[41]</sup> were removed using energy minimization in MOE (same procedure as described above). HELANAL<sup>[54]</sup> was used to analyze the bending angle in transmembrane domains. For the putative escitalopram-binding site, we used the GRID software (v22a)<sup>[55,56]</sup> to calculate the molecular interaction fields (MIF) for the probes C3 (CH<sub>3</sub> methyl), C1 = (sp<sup>2</sup> CH aromatic), N3<sup>+</sup> (sp<sup>3</sup> amine NH<sub>3</sub> cation), O (sp<sup>2</sup> carbonyl O), O: (sp<sup>2</sup> carboxy O), F (organic fluorine atom), Cl (organic chlorine atom), and Na<sup>+</sup> (sodium cation). In these calculations, the protein was considered rigid. The GRID box dimensions were chosen to encompass all relevant residues within the binding cleft resulting in a box size of 19 Å × 17 Å × 16 Å. The grid spacing was set to 0.25 Å; all other

GRID input parameters were set to their default values. The calculated GRID contour maps were then viewed while superimposed on the SERT-escitalopram model using MOE.

In continuation of the present study, we have performed molecular dynamics (MD) simulation studies on the hSERT model in complex with either escitalopram or 5-HT.<sup>[57]</sup> During 7 ns (SERT-escitalopram) or 17 ns (SERT-5-HT) of simulations, we found that the complexes are stable, further indicating that the current model is tenable.

## Results and Discussion

### The overall protein model derived from homology modeling

The final alignment of various SERT sequences to that of the *Aquifex aeolicus* leucine transporter is shown in Figure 1. It gives rise to a sequence identity between LeuT and hSERT of 23%. Table 5 shows that the transmembrane domains TM1, 2,

**Table 4.**

Main geometric parameters of the LeuT X-ray structure and the hSERT models.

	Core regions [%]	Ramachandran plot		
		Allowed regions [%]	Generous, allowed regions [%]	Disallowed regions [%]
LeuT X-ray	94.5	5.5	0	0
hSERT step 1	93.7	5.0	0.7	0.7
hSERT step 3	90.3	8.8	0.5	0.5

3, 6, and 8 have a higher percentage of identity to LeuT than the average value of the whole protein. Interestingly, four of these regions: TM1, 3, 6, and 8 are directly involved in substrate-binding in LeuT, and residues in these regions have also been found important for ligand-binding in the monoamine transporters.<sup>[8]</sup> This observation suggests that the fold and function of this protein region are highly conserved among the transporters. Notably, none of the four helical domains directly involved in substrate-binding in the LeuT X-ray structure has an ideal helix form: TM1 and 6 have unwound regions, whereas TM3 and 8 are bent (29° and 22°, respectively) at the ligand-binding site, and one or more hydrogen bonds are lost in the helix compared to the ideal. In the glutamate transporter X-ray structure, a similar arrangement with unwound and bent helices in the ligand-binding site is observed, and these structural conformations are important for transporter function.<sup>[22,58,59]</sup> It is noteworthy that some residues contributing to the structural organization at the ligand-binding site in LeuT are not conserved between the Na<sup>+</sup>/Cl<sup>-</sup>-dependent transporters, and structural heterogeneity is found particularly in the network bringing these regions together (cf. Table 3). We have therefore allowed conformational changes in the analogous regions in the SERT model during the modeling procedure. The backbone conformation of the modified regions of TM1, 3, 6,

and 8 in the initial homology model as obtained in step 1 (Figure 2) and in the final model from step 3 is compared in Figure 3. Some structural changes occur in all four domains. Compared to the step 1 model, the unwound regions of TM1

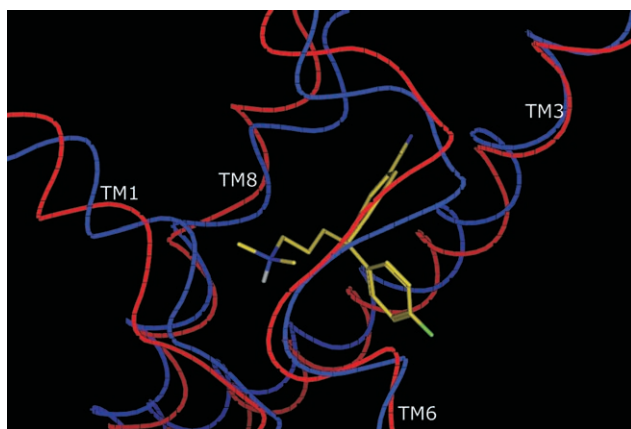


**Figure 3.** Comparison of the backbone conformation in the hSERT models obtained in step 1 (blue) and step 3 (red). For clarity, only the backbones of TM1, 3, 6, and 8 are shown in the ligand-binding cleft. Escitalopram is displayed in stick form.

and 6 are moved slightly away from the ligand in the final model. In addition, the positions of TM1 residues located N-terminal to W103 are changed, which we ascribe to a slight rotation of the helix ( $46^\circ$  toward the N-terminal). The most drastic changes occur in TM6. On average, residues located in the nonconserved coil region in TM6 are moved  $2 \text{ \AA}$  away from the ligand, giving rise to a deformation of this region. The positions of TM3 and 8 residues in vicinity of the ligand-binding site are also changed, apparently due to backbone displacements ( $\sim 1.5\text{--}2 \text{ \AA}$  for  $C_\alpha$  atoms). Superimposition of all  $C_\alpha$  atoms in hSERT and LeuT gives an RMSD of  $2.6 \text{ \AA}$ . Despite these conformational changes, the geometry of the homology model is still acceptable, cf. Table 4, with geometric parameters similar to those for the LeuT-X-ray structure and the initial apo hSERT homology model from step 1. Outliers in the Ramachandran plot were associated with residues located in intra- or extracellular loop regions (EC2-residue R241 and EC5-residue F483). As shown in Table 5, the intra- and extracellular loop regions are less conserved between the transporters, and comprise the regions that because of their flexible nature are most prone to crystal packing effects.

Our final homology model is shown in Figure 4. Escitalopram is docked into a site located in the middle of the membrane-spanning regions, where it is in direct contact with residues from TM1, 3, 6, and 8. In our model, two sodium ions, Na1 and Na2, are located next to the ligand in positions corresponding to those in the LeuT X-ray structure.<sup>[22]</sup> Na1 is located next to the ligand amino group, whereas the position of Na2 is proximal to the cyclic ether of the ligand. Residues involved in the coordination of these two sodium ions are not entirely conserved between LeuT and hSERT. MD simulations have indicated that the sodium-binding sites in our model are stable.<sup>[57]</sup>

**Table 5.** Comparison of the amino acid sequences of LeuT and hSERT.

Domain <sup>[a]</sup>	SERT-LeuT sequence [%] <sup>[b]</sup>
N-terminus	33
TM1	38
EC1	100
TM2	48
IC1	11
TM3	26
EC2	11
TM4	0
IC2	40
TM5	16
EC3	33
TM6	57
IC3	0
TM7	12
EC4	18
TM8	29
IC4	0
TM9	22
EC5	0
TM10	18
IC5	5
TM11	12
EC6	33
TM12	3
C-terminus	-
Entire protein	23

[a] Transmembrane domain (TM), extracellular loop region (EC), intracellular loop region (IC). [b] Numbers refer to the percent of conserved residues within a region defined in the first column. Positions with gap in any of the two sequences are neglected in the calculation.

### Ligand-binding pocket shape

Although the overall sequence identity between LeuT and the monoamine transporters is low, the sequence identity is 57% within a  $5 \text{ \AA}$  radius of the leucine ligand in LeuT, in our emerging model, *vide infra*. As shown in Table 1, some residues at the active site have different properties both with respect to size, geometry, and physical properties in hSERT and LeuT. Some of these residue differences and their relation to differences in substrate properties are discussed below. We primarily observe differences at the six LeuT/hSERT positions N21/Y95, G24/D98, Y108/Y176, T254/S336, S256/G338, and I359/G442, as summarized in Table 6 and discussed briefly in the following.

The significant side chain size difference at positions I359/G442 has previously been linked to volume differences in substrates.<sup>[22]</sup> The residue is relatively small in transporters of larger substrates such as serotonin, but large in transporters of smaller substrates such as leucine. Similar relationships are likely to be observed for inhibitors. In our model, the central part of the ligand fluorophenyl group is located right on top of the G442  $C_\omega$  such that inhibitor binding would not be possible in G442 mutants. Residue differences at positions LeuT/hSERT T254/S336 might also be related to the ligand type. In the LeuT X-ray crystal structure, the side chain of this residue is also involved in a hydrogen bond with the ligand amine group. In the monoamine transporters, the substrate amine adopts a slightly different position to establish the ion-rein-

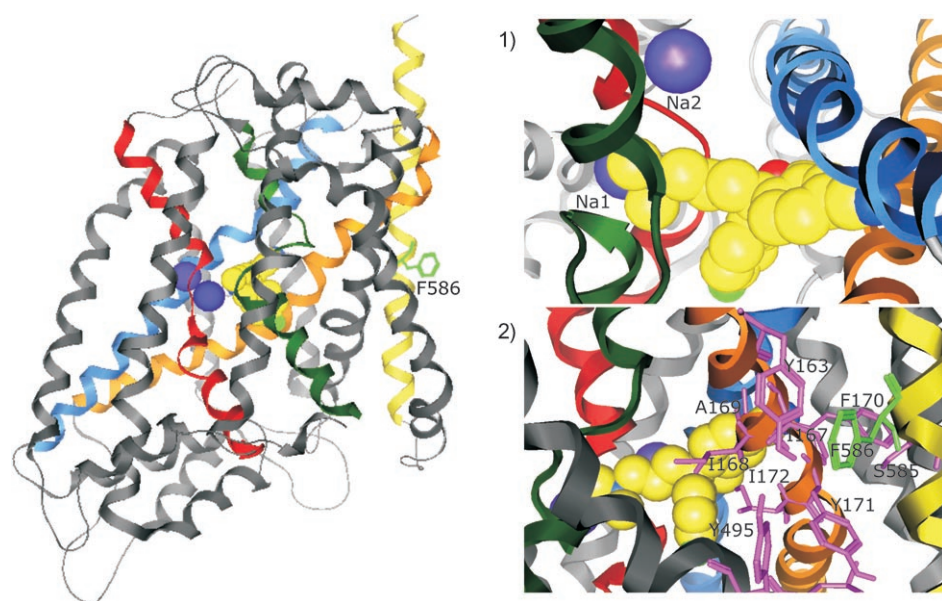


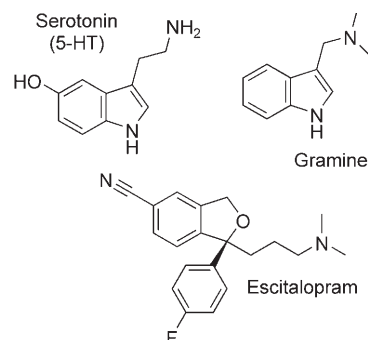
**Figure 4.** Escitalopram-bound hSERT model. The four transmembrane domains, TM1, 3, 6, and 8, that are directly involved in ligand-binding are highlighted in red, orange, green, and blue, respectively. Escitalopram (yellow) is shown in a van der Waals sphere model. The two sodium ions Na1 and Na2 are highlighted in blue. Insert 1 shows the ligand- and sodium-binding pockets. Insert 2 shows the transporter region surrounding F586. Residues between F586 and the escitalopram-binding site are shown in purple. For clarity, the protein orientation in both inserts has been changed relative to the main figure.

forced hydrogen bond with the TM1 aspartate (D98 in hSERT), thereby precluding a contact to S336 (or a corresponding residue in NET and DAT), ultimately causing a different conformation of S336 compared to T254 in LeuT (Table 6). With respect to interhelical hydrogen-bonding networks at the ligand-binding site, we observe differences between the LeuT X-ray structure and our hSERT model (cf. Tables 3 and 6). The changes are mediated by differences in the identities of three pairs of involved residues: in LeuT, there is a TM1–TM6 contact between N21(N $\delta$ ) and S256(OH), whereas the corresponding contact in hSERT spans between Y95(OH) and G338(O). The second contact is between TM1 and TM8, mediated by LeuT N21(O)–S355(OH) or hSERT Y95(O)–S438(OH). The third hydrogen-

bonded contact in LeuT spans between the leucine ligand(O $\delta$ ) and the TM3 residue Y108(OH), whereas the contact in hSERT involves the TM1 residue D98(O $\delta$ ) and the TM3 residue Y176(OH).<sup>[60]</sup>

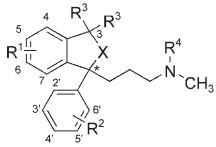
#### Escitalopram-binding pocket

Escitalopram (shown) is a highly specific inhibitor of hSERT, cf. Table 7 ( $K_i$ , 5-HT uptake 13 nM).<sup>[16]</sup> Escitalopram is composed of a cyanophthalane group, a fluorophenyl group, and a dimethylaminopropyl chain, and most of the ligand flexibility is in the propyl linker attached to the dimethylamine group. In the obtained SERT model, the three branches of escitalopram, the dimethylaminopropyl chain, the fluorophenyl, and cyanophthalane groups occupy separate clefts in the



**Table 6.** Differences in contacts in the ligand-binding sites in LeuT and the hSERT model.

Domain	Residue in LeuT	Comment to the residue in LeuT X-ray structure	Residue in hSERT	Comment to the residue in hSERT homology model
TM1	N21	<b>O<math>\delta</math></b> : TM1-6 H-bound contact to S256( <b>H<math>\gamma</math></b> ), pulling TM1 and TM6 together at the ligand-binding cleft. <b>O</b> : TM1-8 contact to S355( <b>H<math>\gamma</math></b> ).	Y95	<b>HH</b> : TM1-6 contact to G338( <b>O</b> ) pulling TM1 and TM6 together at the ligand-binding cleft. <b>O</b> : TM1-8 contact to S438( <b>H<math>\gamma</math></b> ).
TM1	G24	Small residue provides space for leucine carboxy group.	D98	<b>O<math>\delta</math></b> : contact with ligand N. Both <b>O<math>\delta</math></b> 's of D98 carboxy group located in same positions as <b>O</b> 's in leucine in LeuT.
TM3	Y108	<b>HH</b> : contact to leucine <b>O<math>\delta</math></b> .	Y176	<b>HH</b> : see entry D98( <b>O<math>\delta</math></b> ).
TM6	T254	<b>O</b> : contact to leucine <b>N</b> . Unusual rotamer ( $\chi_1 = -163^\circ$ ).	S336	No ligand contact. Usual rotamer ( $\chi_1 = -66^\circ$ ).
TM6	S256	<b>O<math>\gamma</math></b> : contact to leucine <b>N</b> . <b>H<math>\gamma</math></b> : see entry N21.	G338	<b>O</b> : see entry Y95( <b>HH</b> ).
TM8	S355	<b>H<math>\gamma</math></b> : see entry N21.	S438	<b>H<math>\gamma</math></b> : see entry Y95( <b>O</b> ).
TM8	I359	<b>side chain</b> : contact to leucine.	G442	small residue provides space for ligand.

**Table 7.** Activities of citalopram analogues.


Compound	Chirality	X	R <sup>1</sup>	R <sup>2</sup>	R <sup>3</sup>	R <sup>4</sup>	5-HT uptake inhibition IC <sub>50</sub> [nM]
1. Escitalopram	S	O	5-CN	4'-F	H	CH <sub>3</sub>	1.8 <sup>[a]</sup>
2. <i>R</i> -citalopram	R	O	5-CN	4'-F	H	CH <sub>3</sub>	210 <sup>[a]</sup>
3. Citalopram	racemic	O	5-CN	4'-F	H	CH <sub>3</sub>	14 <sup>[b]</sup>
4.	racemic	O	H	H	H	CH <sub>3</sub>	600 <sup>[b]</sup>
5.	racemic	O	H	4'-F	H	CH <sub>3</sub>	140 <sup>[b]</sup>
6.	racemic	O	H	4'-Cl	H	CH <sub>3</sub>	110 <sup>[b]</sup>
7.	racemic	O	5-F	H	H	CH <sub>3</sub>	230 <sup>[b]</sup>
8.	racemic	O	5-Cl	H	H	CH <sub>3</sub>	220 <sup>[b]</sup>
9.	racemic	O	5-Cl	4'-Cl	H	CH <sub>3</sub>	20 <sup>[b]</sup>
10.	racemic	O	5-Cl	4'-CN	H	CH <sub>3</sub>	29 <sup>[b]</sup>
11.	racemic	O	5-CF <sub>3</sub>	4'-CN	H	CH <sub>3</sub>	24 <sup>[b]</sup>
12.	racemic	O	5-CN	4'-Cl	H	CH <sub>3</sub>	17 <sup>[b]</sup>
13.	racemic	O	5-CN	4'-CN	H	CH <sub>3</sub>	29 <sup>[b]</sup>
14. Talopram <sup>[c]</sup>	racemic	O	H	H	CH <sub>3</sub>	H	1400 <sup>[d]</sup>
15. Talsupram <sup>[c]</sup>	racemic	S	H	H	CH <sub>3</sub>	H	850 <sup>[d]</sup>

[a] human brain synaptosomes (Lundbeck screening database). [b] rabbit blood platelets.<sup>[68]</sup> [c] NET: K<sub>i</sub> talopram: 6.4 nM and talsupram 2.5 nM.<sup>[74]</sup> [d] rat brain synaptosomes.<sup>[75]</sup>

protein (Figure 5). In the cleft surrounding the dimethylaminopropyl chain, the ligand–amine D98 ion-reinforced hydrogen bond contributes to the electrostatic stabilization, whereas the interactions between one of the ligand N-methyl groups and F335, the propyl chain and F341, and the propyl chain and Y95 contribute to the hydrophobic stabilization. The fluorophenyl group is stabilized in its binding pocket by three kinds of interactions: electrostatic contacts (fluorine to Y175 hydroxy group),  $\pi$ - $\pi$  stacking (ligand-phenyl to Y176), and hydrophobic contacts (ligand-phenyl to I172  $\delta$ -methyl group). The cyanophthalane group is stabilized by 1) weak electrostatic contacts involving the partially positively charged carbon atom in the cyano group and the backbone carbonyl of A169, and 2) hydrophobic interactions between the ligand phthalane group

and the  $\delta$ -methyl group of I172 and G442 (Figure 5). In the following, residues directly involved in ligand binding are discussed in relation to mutagenesis studies and results from pharmacophore modeling approaches.

**D98**

Residue D98 is expected to be involved in an ion-reinforced hydrogen bond to the native substrate and inhibitors.<sup>[33]</sup> Indeed, in our model, D98 forms electrostatic contacts with the amine group of escitalopram, while also coordinating to a sodium ion that is in the same location as the sodium ion Na1 in LeuT. The importance of residue D98 for transporter function and inhibition has been known for some time, and D98 has been the subject of several site-directed mutagenesis studies.<sup>[33]</sup> If G, A, N, or T is introduced at this position, the transporter is essentially inactive.<sup>[33]</sup> None of these residues can stabilize the protein–ligand complex by a salt bridge. Interestingly, a D98E mutant cannot couple 5-HT transport to the sodium gradient across the plasma membrane (rSERT:  $K_M$  Na<sup>+</sup> D98E > 100 000 nM;  $K_M$  Na<sup>+</sup> wild type 19 900 nM). Instead of favoring serotonin as a substrate, this mutant prefers the shorter substrate gramine (rSERT:  $K_M$  gramine D98E 810 nM;  $K_M$  gramine wild type 10 300 nM). This is not surprising, because the glutamic acid side chain is longer than the aspartic acid side chain by one methylene group. Consequently, in the D98E mutant, there is limited space in the binding pocket for the ethylamino group

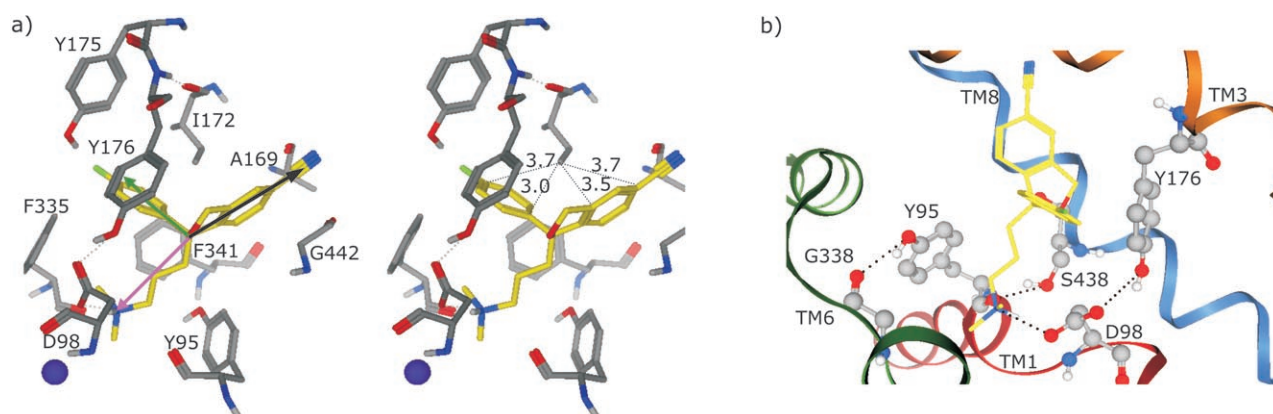


**Figure 5.** a) Stereoview of the escitalopram-binding site in hSERT. The ligand is highlighted in yellow. The three subpockets harboring the dimethylaminopropyl part of the ligand, the fluorophenyl part, and the cyanophthalane skeleton are indicated by purple, green, and black arrows, respectively. The gray dashed lines represent the ion-reinforced hydrogen bond between D98, the ligand amino group and the Y176–D98 contact. The black dashed line and the corresponding distances indicate the distances (Å) between the I172  $\delta$ -carbon and ligand atoms. b) Hydrogen-bonding network in the escitalopram-binding site. The three interhelical hydrogen-bonding interactions and the D98–ligand contact are highlighted by dashed lines.



of 5-HT. Based on our three-dimensional model, the D98E carboxyl group would be positioned deeper into the binding cleft and cannot interact with both the substrate (amine) and the sodium ion. This is probably why a diminished sodium-substrate coupling is observed for D98E. The D98E mutant has also been analyzed with respect to inhibitor binding, and it has been found that racemic citalopram also exhibit reduced affinity to the mutant (rSERT:  $K_i$  citalopram D98E 270 nM;  $K_M$  citalopram wild type 2.2 nM).<sup>[33]</sup> This fits well with the constructed model, where limited space is available for citalopram with an extended side chain at position 98.

During the initial modeling procedure, we observed that residue D98 could adopt two different conformations. However, only one of these rotamers (dihedral angle N-C $_{\alpha}$ -C $_{\beta}$ -C $_{\gamma}$  of 65°) point the side chain inward toward the ligand-binding site where it establishes contact with Na1 and the ligand amine simultaneously. According to a rotamer library, this conformation is the less populated.<sup>[61]</sup> However, this conformation is essential for obtaining the proposed protein–ligand salt bridge.<sup>[33]</sup>

### Y95

During the initial modeling procedure, we observed that the phenol side chain of residue Y95 could either point inward towards the ligand-binding site or outward towards the extracellular surface. Based on the two observations that the corresponding residue N21 in the LeuT X-ray structure point inward towards the ligand-binding site,<sup>[22]</sup> and hSERT mutagenesis studies have identified this residue as important for escitalopram binding,<sup>[18,46,49,62]</sup> we selected the homology model, where the residue pointed inwards and thereby interacted with G338. This gives rise to an interhelical contact between TM1 and 6 (similar to the N21-to-S256 mediated contact in LeuT, see Table 6) and a hydrophobic contact between Y95 and the escitalopram propyl chain. The hydrogen-bonding network between TM1 (Y95) and 6 (G338) seems to stabilize the protein–ligand interaction by maintaining Y95 in a position suitable for ligand contacts. In line with this hypothesis, escitalopram displays a 19-fold decrease in affinity towards the mutant Y95F<sup>[18]</sup> which lacks the hydroxy group and therefore cannot be involved in the hydrogen-bonding network.

### A169, I172, and F586

Based on species variations in ligand affinity, hSERT residues A169, I172, and F586 have been found to be important for inhibitor binding.<sup>[16]</sup> Larsen and co-workers have reported that escitalopram has a lower (41-fold) affinity for gSERT compared to hSERT. They have linked this difference in affinity to the changes at three positions between hSERT and gSERT: A169D, I172V, and F586I. By introducing hSERT residues in gSERT at these three positions, affinities similar to those observed in hSERT could be achieved and vice versa.<sup>[16]</sup> In our model, the I172  $\delta$ -methyl group establishes hydrophobic contact with both aromatic groups of escitalopram, see Figure 5a. Therefore, this interaction seems important for escitalopram binding. Consequently, the reduced affinity of escitalopram towards

I172V, which lacks the  $\delta$ -methyl group, is in good agreement with our model. Similarly, escitalopram binding is diminished in I172M.<sup>[18]</sup> In our model, a methionine at this position would most probably give rise to steric clashes with the ligand.

As shown in Figure 5a, residue A169 is located next to the escitalopram cyano group. The A169D mutation results in a reduced affinity for escitalopram, probably due to electrostatic repulsion between the ligand and A169D.

F586 is located in TM12, which is more than 14 Å away from the ligand-binding site in our model (Figure 4). Based on our model, only an indirect effect of F586 on the ligand-binding site is possible as a comprehensive mutagenesis study has suggested previously.<sup>[63]</sup> In our model, we observe that the F586 side chain is part of a tight hydrophobic network with aromatic residues surrounding the ligand (not shown).<sup>[64]</sup>

### Y175, Y176, F335, and F341

Several other residues involved in ligand- and substrate-binding are highly conserved in sodium-chloride dependent neurotransmitter transporters, including Y175, Y176, F335, and F341. Mutagenesis studies have identified the first two residues as important for transporter function.<sup>[50]</sup> The current model might explain the structural basis for this finding. Y176 binds via its hydroxy group to the one D98 acid carbonyl oxygen atom, which is not involved in the protein–ligand salt bridge. A corresponding interaction is found in LeuT, where the tyrosine residue Y108 interacts with one of the substrate oxygen atoms. In our model, the Y175 hydroxy group establishes an electrostatic contact with the fluorine atom of escitalopram. At the current stage, it is not clear how important this putative contact is for ligand binding.<sup>[65]</sup>

F335 delimits the depth of the pocket into which one of the escitalopram amine methyl groups is buried, (Figure 5a). This is in line with results from structure–activity relationships of various compound classes, indicating that there is only limited space near the binding site for the escitalopram amine group.<sup>[66,67]</sup> As shown in Figure 5a, F341 interacts weakly with two ligand structural components: the propyl chain (hydrophobic interactions) and the fluorophenyl group ( $\pi$ - $\pi$  interactions). To further elucidate the role of the two phenylalanines, mutational studies combined with affinity measurements are being pursued.

### Ligand structure–activity relationships

Based on a citalopram compound series, structure–activity relationships (SAR) have been established for the serotonin transporter.<sup>[10,68,69]</sup> In the following, the results from these studies are discussed in relation to the escitalopram-binding site in our putative hSERT model. Our hSERT model can explain SAR tendencies in the citalopram compound series. For other ligand classes, it is possible that the ligand-binding site conformation has to be changed slightly to adopt to the ligands.<sup>[62]</sup>

Gain or loss of SERT affinity has been linked to the substitution pattern in the two aromatic rings. It has been observed (Table 7) that electron-withdrawing substituents in positions

C4' and C5 contribute most to the enhancement of biological activity. Analogue **4**, lacking such substituents, displays relatively low affinity towards SERT, whereas some affinity is gained in compounds having an electron-withdrawing substituent at either position C4' (compounds **5** and **6**) or C5 (compounds **7** and **8**). However, affinities comparable to that of (es)citalopram are only achieved if substituents are introduced at C4' as well as C5 (compare **1** and **3** with **9–13**). Electron-withdrawing substituents are required for high affinity. Almost equal activities are associated with F, Cl, CF<sub>3</sub>, and CN at position C5, and F, Cl, and CN at position C4' in various combinations. The transporter, however, seems very restrictive with respect to substitution position. The gain in activity compared to compound analogues lacking electron-withdrawing substituents is primarily achieved by introducing substituents at positions C4' and C5. Substituents at positions 2', 6, and 7 tend to either improve very little or even decrease activity (not shown).<sup>[68]</sup> To study how our hSERT model can explain such restricted substitution patterns, we calculated the molecular interaction field using GRID.<sup>[55,56]</sup> Figure 6 shows MIFs for the ligand-binding site constructed using either a hydrophobic

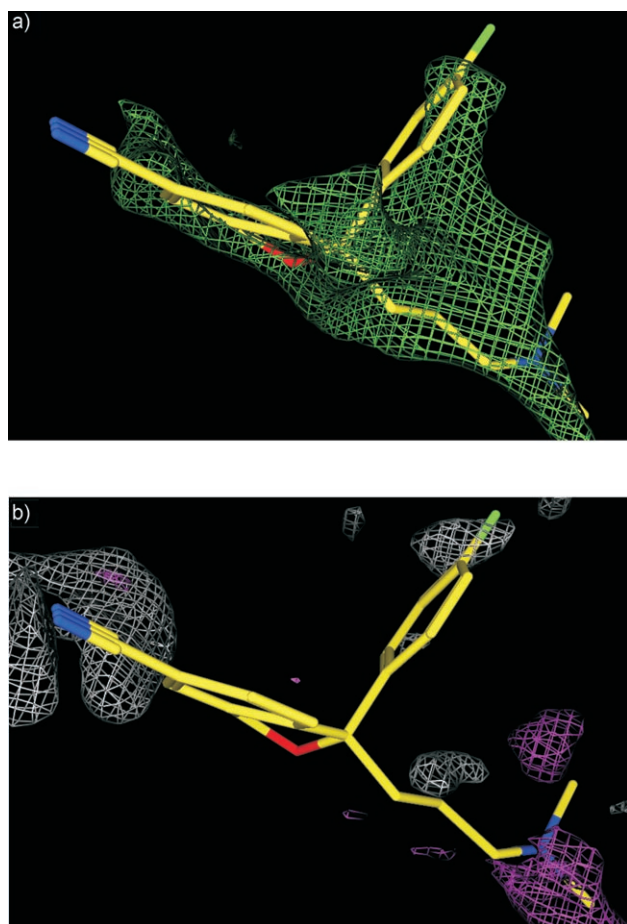


**Figure 6.** GRID maps showing the most favorable positions of various kinds of groups in the binding cleft. The ligand is shown in stick form. Map for a) the hydrophobic C3 probe (green) at energy level  $-3.00 \text{ kcal mol}^{-1}$ , and b) the positively charged  $\text{N}3^+$  probe (magenta) at energy level  $-15.55 \text{ kcal mol}^{-1}$ , and the organic fluorine probe F (white) at energy level  $-3.00 \text{ kcal mol}^{-1}$ .

(C3), a charged nitrogen ( $\text{N}3^+$ ), or an organic fluorine (F) probe. Hydrophobic protein–ligand interactions occur in the central part of the binding pocket that is occupied by the three hydrophobic parts of escitalopram (propyl chain, phthalane moiety, and phenyl group), whereas a favorable position for a positively charged nitrogen atom is predicted exactly where the amine nitrogen atom in escitalopram is located (Figure 6b). According to the organic fluorine MIF, the partially negatively charged fluorine atom would prefer to be located in two regions closely corresponding to the positions of the cyano group at C5 and/or the fluorine substituent at C4'. Based on the agreement between SAR and our GRID predictions, we conclude that our putative hSERT model can explain the SAR for the citalopram compound series.

Future studies will address the transporters of dopamine (DAT) and norepinephrine (NET). However, at the present time, we can rationalize from our hSERT model some SERT/DAT/NET specificities. According to the SSRI pharmacophore model, substituents at carbon 5 are essential for obtaining SERT selectivity over DAT and NET.<sup>[10]</sup> In our model, we notice that the nonconserved (between the monoamine transporters) residue hSERT L443 is located in the vicinity of the cyano group substituent at C5. In DAT and NET, a methionine is located at the corresponding position, providing less space for C5 substituents than in SERT. Two selective NET compounds talopram (**14**) and talsupram (**15**) are also members of the citalopram compound series. The methyl substituents at C3 in these two analogues would interfere adversely with Y176 (conserved in the monoamine transporters) and T439 in our hSERT model, consistent with the finding that **14** and **15** display highly reduced affinity to SERT.

### Allosteric site

In this initial stage of model development, we focused on escitalopram. Its disteromer displays much weaker affinity for the primary site ( $K_{\text{iv}}$  5-HT uptake  $394 \text{ nM}$ ).<sup>[16]</sup> This difference in binding affinity has previously been explained by the SERT pharmacophore model.<sup>[10]</sup> The superior performance in terms of efficacy and onset of action of escitalopram compared to the racemic mixture of citalopram (Cipramil, Celexa) has been ascribed to hSERT allosteric effects.<sup>[70,71]</sup> Escitalopram stabilizes its own binding to the primary binding site by activating/binding to a low-affinity allosteric site. *R*-citalopram also binds to that site, but its stabilizing effects on the escitalopram-bound primary site are reduced in comparison with escitalopram.<sup>[22]</sup> Mutagenesis studies have identified several residues important for allosteric modulation.<sup>[24–26]</sup> As shown in Figure 7a, these residues cluster on the membrane-facing surfaces of TM10, 11, and 12. A tight hydrophobic network (Figure 7b) links some of these residues to residues in the vicinity of the escitalopram-binding site. Further modeling may help to unravel the details of how ligands interact with this site and to explain a possible link between allosteric stabilization and transporter dimerization.<sup>[27]</sup>

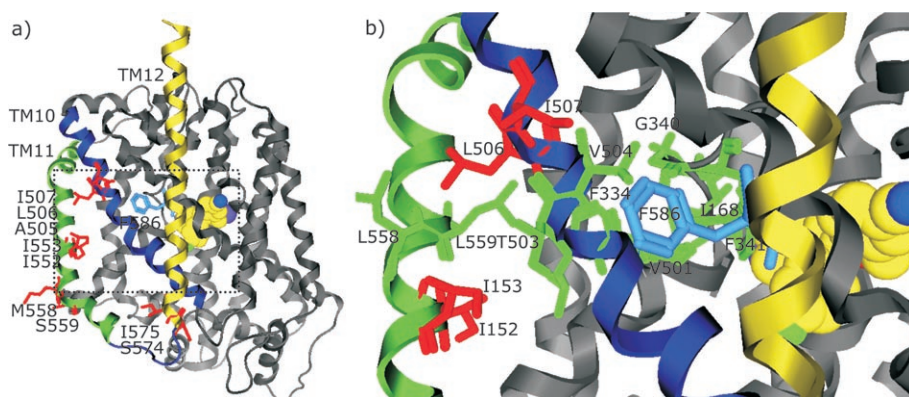


**Figure 7.** a) Putative allosteric region.<sup>[73]</sup> Residues important for escitalopram allosteric stabilization of escitalopram-bound hSERT are illustrated in red cap sticks. These are located in transmembrane domains TM10 (blue), TM11 (green), and TM12 (yellow). F586 is shown in blue. Escitalopram is shown in yellow at the primary site. b) Residues involved in the putative hydrophobic network between the allosteric region and the primary ligand-binding site are highlighted in green.

## Acknowledgements

G.H.P. acknowledges financial support from the Danish National Research Foundation via a grant to MEMPHYS-Center for Biomembrane Physics. A.M.J. acknowledges H. Lundbeck A/S and the Ministry for Science, Technology and Innovation for an Industrial PhD scholarship. Figures were prepared in MOE.<sup>[41]</sup>

**Keywords:** escitalopram · homology modeling · molecular recognition · serotonin transporter · structure–activity relationships

## Conclusions

Predicting the three-dimensional structure of proteins from their amino acid sequence is challenging but important for improving the understanding of protein structure–function relationships. This is of special interest for the group of membrane-bound proteins. They represent biological targets for the majority of drugs, but the lack of X-ray structures for most of these proteins render it impossible to obtain direct insight into their 3D structure.<sup>[72]</sup> For the Na<sup>+</sup>/Cl<sup>−</sup>-dependent neurotransmitter transporter family for which only one template structure is available, homology modeling is the most obvious strategy to obtain a structural model of another NSS member. We used the X-ray structure of the leucine amino acid transporter, LeuT, as a template for developing a homology model for the serotonin endogenous amine transporter, hSERT in complex with the SSRI escitalopram. In the evolution of the model, we have included both information from mutational studies affecting functionality<sup>[8, 16–18]</sup> and pharmacophore modeling results.<sup>[10]</sup>

In the final model, escitalopram is anchored in the binding cleft by an ion-reinforced hydrogen bond between the protonated ligand amine and D98 and by several hydrophobic contacts, including contacts between the aromatic parts of the ligand and residues I172, F341, G442, and Y176. In addition, the escitalopram dimethylaminopropyl chain is in contact with residues Y95 and F335.

Several of the involved residues have been characterized by mutagenesis studies, and we find that the obtained hSERT-escitalopram model can explain observed transporter selectivity with respect to inhibitor binding for a number of mutated SERT amino acid positions. In addition, our model is in agreement with structure–activity relationships determined for a citalopram series of compounds. The binding of other reuptake inhibitors to SERT, NET, and DAT, and how they mechanistically interfere with the transport mechanism are currently under investigation.

- [1] C. Sanchez, K. P. Bøgesø, B. Ebert, E. H. Reines, C. Bræstrup, *Psychopharmacology* **2004**, *174*, 163–176.
- [2] L. Iversen, *Mol. Psychiatry* **2000**, *5*, 357–362.
- [3] M. J. Owens, C. B. Nemeroff, *Clin. Chem.* **1994**, *40*, 288–295.
- [4] M. J. Owens, W. N. Morgan, S. J. Plott, C. B. Nemeroff, *J. Pharmacol. Exp. Ther.* **1997**, *283*, 1305–1322.
- [5] M. J. Owens, D. L. Knight, C. B. Nemeroff, *Biol. Psychiatry* **2001**, *50*, 345–350.
- [6] R. D. Blakely, H. E. Berson, T. Robert, M. G. Caron, M. M. Peek, H. K. Prince, C. C. Bradley, *Nature* **1991**, *354*, 66–70.
- [7] B. J. Hoffman, E. Mezey, M. J. Brownstein, *Science* **1991**, *254*, 579–580.
- [8] N.-H. Chen, M. E. A. Reith in *Contemporary Neuroscience: Neurotransmitter Transporters: Structure, Function, and Regulation* (Ed.: M. E. A. Reith), Humana, Totowa, **2002**, pp. 53–109.
- [9] J. Pratuangdejikul, B. Schneider, P. Jaudon, V. Rosilio, E. Baudoin, S. Loric, M. Conti, J. M. Launay, P. Manivet, *Curr. Med. Chem.* **2005**, *12*, 2393–2406.
- [10] K. Gundertofte, K. P. Bøgesø, T. Liljefors in *Computer-Assisted Lead Finding and Optimization* (Eds.: H. v. d. Waterbeemd, B. Testa, G. Folkers), Wiley-VCH, Weinheim, **1997**, pp. 443–459.
- [11] A. S. Chang, S. M. Chang, D. M. Starnes, *Eur. J. Pharmacol.* **1993**, *247*, 239–248.
- [12] R. Bureau, C. Daveu, J. C. Lancelot, S. Rault, *J. Chem. Inf. Comput. Sci.* **2002**, *42*, 429–436.
- [13] G. Humber, D. Lee, S. Rakhit, M. Treasurywala, *J. Mol. Graphics.* **1985**, *3*, 84–89.
- [14] A. Rupp, K. A. Kovar, G. Beuerle, C. Ruf, G. Folkers, *Pharm. Acta Helv.* **1994**, *68*, 235–244.
- [15] U. H. Lindberg, S. O. Thorberg, S. Bengtsson, A. L. Renyi, S. B. Ross, S. O. Ogren, *J. Med. Chem.* **1978**, *21*, 448–456.
- [16] M. B. Larsen, B. Elfving, O. Wiborg, *J. Biol. Chem.* **2004**, *279*, 42147–42156.
- [17] L. Norregaard, U. Gether, *Curr. Opin. Drug Discov. Devel.* **2001**, *4*, 591–601.
- [18] L. K. Henry, J. R. Field, E. M. Adkins, M. L. Parnas, R. A. Vaughan, M.-F. Zou, A. H. Newmann, R. D. Blakely, *J. Biol. Chem.* **2006**, *281*, 2012–2023.
- [19] A. W. Ravna, I. Sylte, S. G. Dahl, *J. Pharmacol. Exp. Ther.* **2003**, *307*, 34–41.
- [20] A. W. Ravna, O. Edvardsen, *J. Mol. Graphics Modell.* **2001**, *20*, 133–144.
- [21] A. W. Ravna, I. Sylte, K. Kristiansen, S. G. Dahl, *Bioorg. Med. Chem.* **2006**, *14*, 666–675.
- [22] A. Yamashita, S. K. Singh, T. Kawate, Y. Jin, E. Gouaux, *Nature* **2005**, *437*, 215–223.
- [23] G. Rudnick in *Contemporary Neuroscience: Neurotransmitter Transporters: Structure, Function, and Regulation* (Ed.: M. E. A. Reith), Humana, Totowa, **2002**, pp. 25–52.



- [24] N. R. Goldberg, T. Beuming, O. S. Soyler, R. A. Goldstein, H. Weinstein, J. A. Javitch, *Eur. J. Pharmacol.* **2003**, *479*, 3–12.
- [25] N. R. Goldberg, T. Beuming, H. Weinstein, J. A. Javitch in *Strategies in Molecular Neuropharmacology* (Eds.: A. Schousboe and H. Bräuner-Osborne), Humana, Totowa, **2003**, pp. 213–234.
- [26] Y. Cao, M. Li, S. Mager, H. A. Lester, *J. Neurosci.* **1998**, *18*, 7739–7749.
- [27] S. Pantanowitz, A. Bendahan, B. I. Kanner, *J. Biol. Chem.* **1993**, *268*, 3222–3225.
- [28] L. K. Henry, L. J. DeFelice, R. D. Blakely, *Neuron* **2006**, *49*, 791–796.
- [29] T. Beuming, L. Shi, J. A. Javitch, H. Weinstein, *Mol. Pharmacol.* **2006**, *70*, 1630–1642.
- [30] A. W. Ravna, M. Jaronczyk, I. Sylte, *Bioorg. Med. Chem. Lett.* **2006**, *16*, 5594–5597.
- [31] K. M. Penado, G. Rudnick, M. M. Stephan, *J. Biol. Chem.* **1998**, *273*, 28098–28106.
- [32] G. E. Torres, R. R. Gainetdinov, M. G. Caron, *Nat. Rev. Neurosci.* **2003**, *4*, 13–25.
- [33] E. L. Barker, K. R. Moore, F. Rakhshan, R. D. Blakely, *J. Neurosci.* **1999**, *19*, 4705–4717.
- [34] A. Androutsellis-Theotokis, N. R. Goldberg, K. Ueda, T. Beppu, M. L. Beckman, S. Das, J. A. Javitch, G. Rudnick, *J. Biol. Chem.* **2003**, *278*, 12703–12709.
- [35] A. Bairoch, R. Apweiler, *Nucleic Acids Res.* **1999**, *27*, 49–54.
- [36] H. M. Berman, J. Westbrook, Z. Feng, G. Gilliland, T. N. Bhat, H. Weissig, I. N. Shindyalov, P. E. Bourne, *Nucleic Acids Res.* **2000**, *28*, 235–242.
- [37] J. D. Thompson, D. G. Higgins, T. J. Gibson, *Nucleic Acids Res.* **1994**, *22*, 4673–4680.
- [38] A. Sali, T. L. Blundell, *J. Mol. Biol.* **1993**, *234*, 779–815.
- [39] J. Dunbrack, *Curr. Opin. Struct. Biol.* **2002**, *12*, 431–440.
- [40] R. A. Laskowski, M. W. MacArthur, D. S. Moss, J. M. Thornton, *J. Appl. Crystallogr.* **1993**, *26*, 283–291.
- [41] Molecular Operating Environment, version 2005.06 Chemical Computing Group Inc., Montreal.
- [42] T. A. Halgren, *J. Comput. Chem.* **1996**, *17*, 490–519.
- [43] Y. Smicun, S. D. Campbell, M. A. Chen, H. Gu, G. Rudnick, *J. Biol. Chem.* **1999**, *274*, 36058–36064.
- [44] K. R. Moore, R. D. Blakely, *Biotechniques* **1994**, *17*, 130–135.
- [45] R. D. Blakely, K. R. Moore, Y. Quin in *Molecular Biology and Function of Carrier Proteins* (Eds.: L. Reuss, J. M. Russell, M. L. Jennings), Rockefeller University Press, New York, **1993**, pp. 284–300.
- [46] E. L. Barker, M. A. Perlman, E. M. Adkins, W. J. Houlihan, Z. B. Pristupa, H. B. Niznik, R. D. Blakely, *J. Biol. Chem.* **1998**, *273*, 19459–19468.
- [47] At this modeling stage we also tried to build the hSERT model around escitalopram, using the MOE environment tool.<sup>[41]</sup> In addition, we also tried to use a hSERT template for homology modeling (escitalopram used as a MOE environment), where residues within the ligand-binding site had been mutated to alanine or glycine. However, none of the obtained hSERT models was suitable for the escitalopram-binding site.
- [48] A less comprehensive backbone modification attempt, where flexibility was allowed only in TM1 and TM6, revealed that to obtain sufficient movements of the TM1 and TM6 unwound regions, some flexibility in TM3 and TM8 was also required.
- [49] E. M. Adkins, E. L. Barker, R. D. Blakely, *Mol. Pharmacol.* **2001**, *59*, 514–523.
- [50] J. G. Chen, A. Sachpatzidis, G. Rudnick, *J. Biol. Chem.* **1997**, *272*, 28321–28327.
- [51] MAESTRO version 2005 Schrödinger LLC, Portland.
- [52] W. Sherman, T. Day, M. P. Jacobson, R. A. Friesner, R. Farid, *J. Med. Chem.* **2006**, *49*, 534–553.
- [53] W. L. Jorgensen, J. Tirado-Rives, *Proc. Natl. Acad. Sci. USA* **2005**, *102*, 6665–6670.
- [54] M. Bansal, S. Kumar, R. Velavan, *J. Biomol. Struct. Dyn.* **2000**, *17*, 811–819.
- [55] P. Goodford, in *Molecular Interaction Fields* (Ed.: G. Cruciani), Wiley-VCH, Weinheim, **2006**, pp. 3–26.
- [56] GRID version 22a 2006 Molecular Discovery Ltd., Middlesex.
- [57] A. M. Jørgensen, L. Tagmose, A. M. M. Jørgensen, K. P. Bøgesø, G. H. Peters, *ChemMedChem* **2007**, *6*, 827–840.
- [58] D. Yernool, O. Boudker, Y. Jin, E. Gouaux, *Nature* **2004**, *431*, 811–818.
- [59] Such a nonideal topology/geometry is expected to be important for 1) providing room for a ligand, 2) offering multiple protein–ligand and protein–sodium ion interactions involving backbone and side-chain atoms, and 3) inducing required conformational changes during the transport cycle.<sup>[22]</sup>
- [60] Despite one or both of the anchoring points for the three contacts differing between the two transporters, a comparison of our putative model with the LeuT X-ray structure reveals that similar architectures are maintained. In fact, the TM1–6 and TM1–8 contacts stretch over the same number of covalent bonds (measured backbone-to-backbone) and provide similar interhelical distances (measured as C–C distances).
- [61] S. C. Lovell, J. M. Word, J. S. Richardson, D. C. Richardson, *Proteins* **2000**, *40*, 389–408.
- [62] L. K. Henry, E. M. Adkins, Q. Han, R. D. Blakely, *J. Biol. Chem.* **2003**, *278*, 37052–37063.
- [63] E. L. Barker, R. D. Blakely, *Mol. Pharmacol.* **1996**, *50*, 957–965.
- [64] F586 is also located in the same part of the transporter as residues proven to be important for transporter dimerization.<sup>[76]</sup> As shown in Figure 7, it is not located directly on the putative dimerization surface, but it might play a role as a link between the dimerization surface and the primary ligand-binding site.
- [65] During the model building, we observed that Y175 can adopt two conformations –pointing inward towards the ligand-binding site or outwards. We selected the inward-pointing rotamer.
- [66] K. P. Bøgesø, *Drug hunting: The medicinal chemistry of 1-piperazino-3-phenylindans and related compounds*, H. Lundbeck A/S, Copenhagen, **1998**.
- [67] K. P. Bøgesø, J. Hyttel, V. Christensen, J. Arnt, T. Liljefors, *Chirality as determinant for neuroleptic or antidepressant action of drugs*, Elsevier, Amsterdam, **1986**.
- [68] A. J. Bigler, K. P. Bøgesø, A. Toft, V. Hansen, *Eur. J. Med. Chem.* **1978**, *12*, 289–295.
- [69] K. P. Bøgesø, B. Bang-Andersen in *Textbook of Drug Design and Discovery* (Eds.: P. Krosgaard-Larsen, T. Liljefors, U. Madsen), Taylor & Francis, London, **2002**, pp. 299–327.
- [70] F. Chen, M. B. Larsen, C. Sanchez, O. Wiborg, *Eur. Neuropsychopharmacol.* **2005**, *15*, 193–198.
- [71] M. El Mansari, O. Wiborg, O. Mnie-Filali, N. Benturquia, C. Sánchez, N. Haddjeri, *Int. J. Neuropsychopharmacol.* **2007**, *10*, 31–40.
- [72] J. P. Rosenbusch, *J. Struct. Biol.* **2001**, *136*, 144–157.
- [73] H. A. Neubauer, C. G. Hansen, O. Wiborg, *Mol. Pharmacol.* **2006**, *69*, 1242–1250.
- [74] J. McConathy, M. J. Owens, C. D. Kilts, E. J. Malveaux, V. M. Camp, J. R. Votaw, C. B. Nemeroff, M. M. Goodman, *Nucl. Med. Biol.* **2004**, *31*, 705–718.
- [75] M. Schou, J. Sovago, V. W. Pike, B. Gulyas, K. P. Bøgesø, L. Farde, C. Hall-din, *Mol. Imaging Biol.* **2006**, *8*, 1–8.
- [76] H. Just, H. H. Sitte, J. A. Schmid, M. Freissmuth, O. Kudlacek, *J. Biol. Chem.* **2004**, *279*, 6650–6657.

Received: October 18, 2006

Revised: February 10, 2007

Published online on April 2, 2007